# Effect of bubble characteristics and nozzle size on the membrane distillation enhanced by gas–liquid two-phase flow

Dashuai Zhang, Xiaopeng Zhang, Li Chen, Wang Lili, Wu Di, Yuqin Xiong, Qiang Lin and Zaifeng Shi

## ABSTRACT

This study investigates the membrane performance and fouling control in bubble-assisted sweeping gas membrane distillation with high concentration saline (333 K saturated solution) as feed. The results show that a longer bubbling interval (3 min) at a fixed bubbling duration of 30 s can most efficiently increase the flux enhancement ratio up to 1.518. Next, the flux increases with the gas flow rate under a relatively lower level, but tends to plateau after the threshold level (1.2 L·min$^{-1}$). Compared to the non-bubbling case, the permeate flux reaches up to 1.623-fold at a higher bubble relative humidity of 80%. It was also found that greater flux enhancement can be achieved and, meanwhile, dramatic flux decline can be delayed for an intermittent bubbling system with a smaller nozzle size. These results accord well with the observations of fouling deposition *in situ* on the membrane surface with scanning electron microscope (SEM).

**Key words** | fouling control, gas–liquid two-phase flow, high concentration saline, membrane distillation

**Dashuai Zhang**
**Xiaopeng Zhang**
**Li Chen**
**Wang Lili**
**Wu Di**
**Yuqin Xiong**
**Qiang Lin**
**Zaifeng Shi** (corresponding author)
Key Laboratory of Water Pollution Treatment & Resource Reuse of Hainan Province,
Hainan Normal University,
Haikou, Hainan 571158,
China
and
College of Chemistry and Chemical Engineering,
Hainan Normal University,
Haikou, Hainan 571158,
China
E-mail: *zaifengshi@163.com*

## INTRODUCTION

Membrane distillation (MD) is an innovative separation technology for desalination, and water and wastewater treatment, due to its merits of mild operation temperature and pressure, with appropriate penetration rate, high rejection rate for nonvolatile components and small footprint when consuming alternative energy sources (Lawson & Lloyd 1997; Jansen *et al.* 2013). Unlike pressure-driven membrane processes such as reverse osmosis (RO), nanofiltration (NF), ultrafiltration (UF), and microfiltration (MF), MD is an emerging thermally driven technology coupled with mass and heat transfer process. Thereby, MD is an appealing method for extra-high concentration brine treatment owing to its insensitivity to feed salinity (Edwie & Chung 2012; Quist-Jensen *et al.* 2016).

However, the decrease of driving force due to concentration and temperature polarization effects as well as fouling/scaling issues impedes the long-term stability performance of MD (Schofield *et al.* 1987; Calabro & Drioli 1997). In the MD process, inorganic fouling (scaling), organic fouling, and biological fouling (biofouling) can be found according to the contaminated material (Gryta *et al.* 2001; Tijing *et al.* 2015). Many optimization strategies have been adopted to minimize the extent of fouling: (a) pretreatment, (b) membrane flushing, (c) gas bubbling, (d) temperature and flow reversal, (e) surface modification for anti-fouling membrane, (f) effect of magnetic/ultrasonic field, (g) use of antiscalants, and (h) chemical cleaning (Nghiem & Cath 2011; Hickenbottom & Cath 2014).



doi: 10.2166/wrd.2019.075

As one of the most promising flux enhancement and anti-fouling techniques, the gas–liquid two-phase flow can induce secondary flow to maximize the shear stress at the membrane surface, displace the concentration and temperature layer, cause pressure pulsing and increase superficial cross-flow velocity (Wibisono *et al.* 2014). Gas sparging technology has been successfully applied to traditional membrane separation technologies (MST) such as MF, UF, and membrane bioreactors (MBRs) (Lu *et al.* 2008; Cerón-Vivas *et al.* 2012). In recent years, there has been a keen interest in the MD process enhanced by gas–liquid two-phase flow for general desalination applications. For instance, Ding *et al.* (2011) observed that the cleaning efficiency of gas bubbling is improved with the increase of gas flow rate and gas bubbling duration, and the decrease of membrane fouling when introducing intermittent gas bubbling during the concentration of traditional Chinese medicines (TCM) by direct contact membrane distillation (DCMD). Chen *et al.* (2013) achieved 26% permeation flux enhancement and later appearance of major flux decline by incorporating gas bubbling into DCMD when salt solution was concentrated from 18% to saturation. Also, it was found that heat-transfer coefficient and temperature polarization coefficient (TPC) reached up to 2.30- and 2.13-fold in comparison with non-bubbling DCMD (Chen *et al.* 2014). A recent air-bubbling vacuum membrane distillation (AVMD) study proposed that the flux was doubled at a certain feed velocity and gas/liquid proportion (Wu *et al.* 2015).

As an extension of the intermittent bubble-enhanced MD process, this paper aims to research the bubble characteristics (i.e., bubble velocity, bubble relative humidity) and nozzle size on mass transfer intensification and scaling mitigation for supersaturated saline solution as feed. Meanwhile, the anti-fouling efficiency in MD brine processing with gas–liquid two-phase can be achieved through the evaluation of the local fouling status on the membrane surface.

## MATERIALS AND METHODS

### Materials and membrane module

Feed solution: saturated NaCl solutions at a temperature of 333 K as feed stream were prepared by magnetically stirring solid sodium chloride (supplied by Guangzhou Chemical Reagent Fac., China) in 1,000 mL of deionized water for 30 min.

A hollow-fiber hydrophobic MD membrane (Jack Co. Ltd, China) was employed in our bubble-assisted sweeping gas membrane distillation (SGMD) experiments. Each membrane is made of polyvinylidene fluoride (PVDF) with 78% porosity, $113 \pm 1.7^{\circ}$ contact angle, 3.07 N breaking strength, 4.038 bar LEPw, 0.22 μm mean pore size, and its inner and outer diameters are 1.2 mm and 0.9 mm, respectively. All data on membrane properties were provided by the manufacturer.

Twenty fibers were placed in parallel in a transparent polypropylene (PC) housing of 230 mm length and 20 mm external surface diameter. The effective fiber length and membrane area in the module are 180 mm and $\sim 1.526 \times 10^{-2}$ m$^2$ separately.

### Experimental set-up

The experimental set-up is shown schematically in Figure 1. The bubble-assisted SGMD system can be divided into two parts: thermal cycle and cooling cycle.

In the thermal cycle, the hot feed, maintained by a heater at constant temperature, was circulated by a self-priming pump. The discharge pressure is manually adjusted by means of a 2/3 way valve on the pump's loop line. The bubble flow introduced by an air pump joins the feed flow at the entrance of the membrane module, and therefore a gas–liquid two-phase flow is injected vertically upward into the membrane module. The velocity and relative humidity (RH) of the bubble is controlled by a gas flow meter and humidifier, respectively. The velocity, temperature, and pressure of feed were individually monitored by temperature indicator (TI), pressure indicator (PI), and rotameter.

In the cooling cycle, condensation water prepared from a cooler is recycled into the condenser pipe. Water vapor turns into water droplets when swept straight down to the condenser pipe by the air pump. The weight and conductivity of the penetrant is measured by a balance and conductivity indicator (CI), respectively. The air pump not only acts as an aid to sweep gas into the membrane module, it also supplies gas bubbling into the feed side. The bubble nozzle mounted at the feed side entrance of the membrane module is used for dispersion of bubbles.

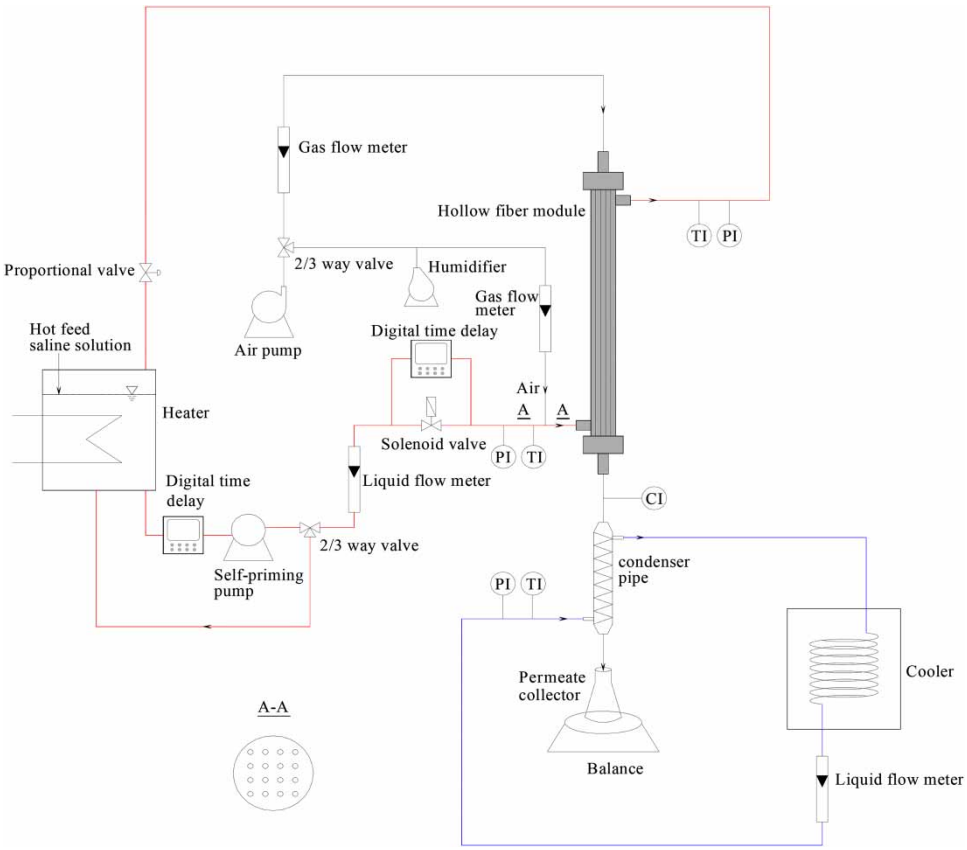


**Figure 1** | Diagram of experimental set-up for bubble-assisted SGMD process.

## Experimental part

In a bubbling system, bubble characteristic is a significant factor for the enhancement process. A series of experiments were conducted to research bubble on/off ratio (30 s/1 min, 30 s/2 min, 30 s/3 min), bubble flow rate ($Q_b$) (0 L/min, 0.4 L/min, 0.8 L/min, 1.2 L/min, 1.6 L/min, 2 L/min), and bubble relative humidity ($RH_b$) (56%, 62%, 68%, 74%, 80%) on the flux enhancement when treated with saturated NaCl solution (333 K) as feed in bubble-assisted SGMD process.

Experiments were also carried out to investigate the effect of different nozzle sizes on the enhancement of critical flux and membrane fouling control. Nozzles with a diameter ($D_n$) of 0 mm, 2.2 mm, 3.5 mm, 6.0 mm, and 10.0 mm were employed to produce bubbles.

All the above experiments were performed under the same operating conditions: feed flow rate ($Q_f$) is 50 $L{\cdot}h^{-1}$, feed inlet temperature ($T_{f\text{-}in}$) on the shell side is 333 K, coolant temperature ($T_c$) is 283 K, gas-sweeping flow rate ($Q_a$) on the lumen side is 0.84 $m^3{\cdot}h^{-1}$, and fill factor ($FF$) is 25.6%. Furthermore, indoor temperature and relative humidity were maintained constant at 26 °C and 74%, respectively, to reduce experimental error.

Regarding experiments of crystal deposition, each set of experiments was run with a new membrane module for a specific time. After the membrane fouling experiment, the membrane module was removed from the apparatus immediately and then put into the constant-temperature oven for drying for 24 h at 303 K. The fouled fibers were cut off at the head and tail, and the middle section used to investigate the status of the pollution situation by scanning electron microscope (SEM).

For the recovery of membrane permeability, routine membrane cleaning was carried out after each bubble-enhanced SGMD experiment without crystal deposition, and the membranes were washed using the following procedure: (1) 30 min acid cleaning with 0.5 wt.% citric acid solution and (2) 1 h flushing by DI water.

### Water quality analyses

The permeation flux ($J$, Kg·m$^{-2}$·h$^{-1}$) in the MD was calculated by Equation (1):

$$J = \frac{\mathrm{m}}{A \times t} \tag{1}$$

where $m$ (Kg) is the weight of permeation, $A$ (m$^2$) is the total effective membrane area, and $t$ (h) is the operation time (Liu *et al.* 2018).

The normalized/relative flux (%) before and after fouling was calculated by Equation (2):

$$J_N = \frac{J_i}{J_0} \times 100\% \tag{2}$$

where $J_0$ (Kg·m$^{-2}$·h$^{-1}$) is the initial flux, and $J_i$ (Kg·m$^{-2}$·h$^{-1}$) is the instantaneous flux during the filtration of real industrial samples, which could cause flux decline due to fouling (García *et al.* 2018).

The energy consumption of the MD system is affected by the membrane, mainly by its thermal energy efficiency ($E$). This parameter evaluates the heat transfer due to flux ($Q_N$ in W m$^{-2}$) and heat total due to conduction through the membrane ($Q$ in W m$^{-2}$) (Eykens *et al.* 2017).

$$E = \frac{Q_N}{Q} \times 100\% \tag{3}$$

The rejection ($R$) of solute was calculated by Equation (4):

$$R = 1 - \frac{c_p}{c_f} \times 100\% \tag{4}$$

The permeate quality is determined by the separation efficiency. In MD it is defined as the retention of non-volatiles in the feed solution and is calculated based on the concentration in feed ($c_f$, g/L) and permeate ($c_p$, g/L) (Eykens *et al.* 2017).

Trans-membrane flux enhancement ratio ($\Phi$) was calculated by Equation (5):

$$\Phi = \frac{J_S}{J_U} \tag{5}$$

where $J_S$ (Kg·m$^{-2}$·h$^{-1}$) is the steady-flow membrane distillation (single-phase flow) flux, and $J_U$ (Kg·m$^{-2}$·h$^{-1}$) is the unsteady-flow membrane distillation (continuous gas–liquid two-phase flow, intermittent gas–liquid two-phase flow with three bubble on/off ratios (30 s/1 min, 30 s/2 min, 30 s/3 min)) flux obtained by different flow regimes samples. The other operating parameters were kept constant.

## RESULTS AND DISCUSSION

### Influence of bubble characteristics on mass transfer

#### Bubble on/off ratio

Figure 2 presents the comparison of trans-membrane flux enhancement ratio ($\Phi$) obtained by different flow regimes: single-phase flow, continuous gas–liquid two-phase flow, intermittent gas–liquid two-phase flow with three bubble on/off ratios (30 s/1 min, 30 s/2 min, 30 s/3 min). The other operating parameters are kept constant. All experiments last for 1 h.

In general, the histogram illustrates that the flux of the bubbling case is above that of the non-bubbling case. The flux enhancement may be attributed to secondary flow by the introduction of bubbling, which promotes the local mixing and increases the superficial cross-flow velocity. Consequently, the temperature/concentration layer at the membrane surface is reduced, and then a higher flux is obtained in a bubbling SGMD process.

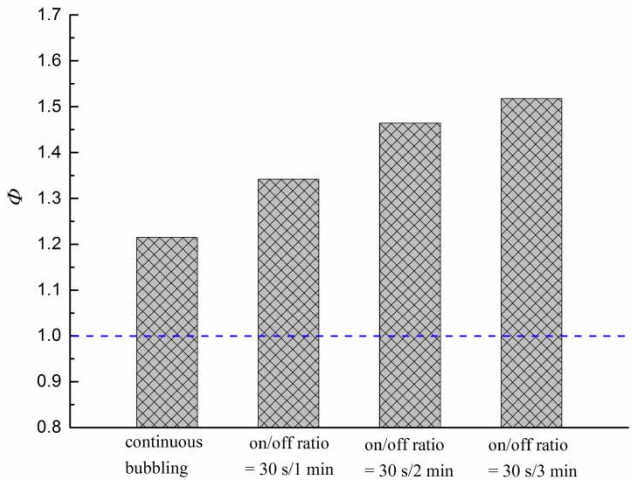


**Figure 2** | Effect of continuous and intermittent gas bubbling on trans-membrane flux (333 K saturated NaCl solution as feed: $Q_f = 50$ L·h$^{-1}$; $T_{f\text{-}in} = 333$ K; $T_c = 283$ K; $Q_a = 0.84$ m$^3$·h$^{-1}$; $FF = 25.6\%$; $Q_g = 0.5$ L·h$^{-1}$; $RH_g = 74\%$; $D_n = 10.0$ mm).

Also, it is observed that the $\Phi$ value of the intermittent bubbling is higher than that of the continuous bubbling (Guibert *et al.* 2002; Cui *et al.* 2003). This may be due to the prolonged occupation of the membrane surface by continuous bubbles, which reduces the effective contact area of feed and membrane surface. Furthermore, some bubbles existing in the membrane pore passages may block the path of water vapor to the permeate side, resulting in a declining trans-membrane driving force. Additionally, $\Phi$ is increased from 1.215 to 1.518 with an increase in the bubbling interval from 1 to 3 min during a settled bubbling duration of 30 s. More feed passes through the module per unit time if the bubbling interval increases, i.e., the stranded bubbles can be duly taken away from the module with the aid of fluid. That makes the upward bubbles flow along the membrane surface together with the feed flow to create moderate shear stress and feed mixing. However, if the bubbling interval is extended for too long, the fouling issue will be more serious. Accordingly, within certain bubble intervals, a higher trans-membrane flux enhancement is longer at a longer bubble interval.

## Bubble flow rate

A series of experiments with and without intermittent gas bubbling were conducted at relatively low feed flow rate (20, 30, 40, 50 $L{\cdot}h^{-1}$) for a 60-min experiment time. During the intermittent bubbling experiments, the effect of different gas flow rates (0.4, 0.8, 1.2, 1.6, 2.0 $L{\cdot}min^{-1}$) on permeate flux were investigated. Experimental results are shown in Figure 3.

Clearly, four $J$ curves follow a similar trend, i.e., the $J$ initially increases with increasing gas flow rate ($0 \leq Q_g \leq 1.2$ $L{\cdot}min^{-1}$) and then reaches a plateau at higher gas flow rate ($1.2 < Q_g \leq 2.0$ $L{\cdot}min^{-1}$). The reason for the increase may be due to the improvement of mass/heat transfer process induced by bubbles. With the local mixing and surface shear force intensified by bubbling, the thinner temperature/concentration boundary layer results in an increase of partial pressure gradient. Therefore, the permeation flux increases correspondingly. However, when the feed flow rate is fixed at 20, 30, 40, 50 $L{\cdot}h^{-1}$, respectively, the flux remains on a stationary value from 1.80 to 2.03 $L{\cdot}m^{-2}{\cdot}h^{-1}$ at the gas flow rate range from 1.2 to 2.0 $L{\cdot}min^{-1}$. This

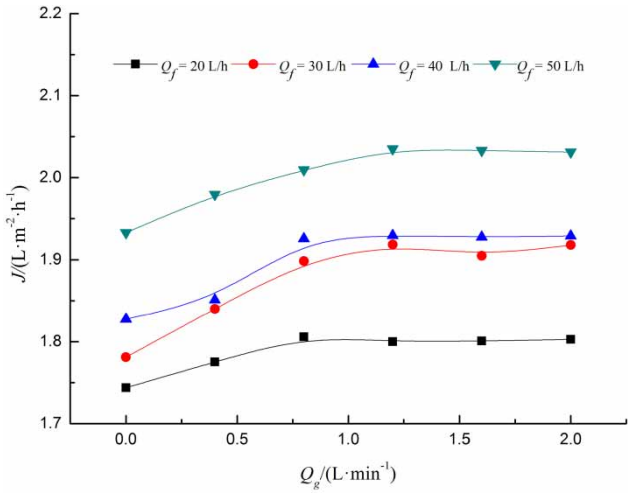


**Figure 3** | Effect of bubble flow rate on trans-membrane flux (333 K saturated NaCl solution as feed: $T_{f\text{-}in} = 333$ K; $T_c = 283$ K; $Q_a = 0.84$ $m^3{\cdot}h^{-1}$; $FF = 25.6\%$; $RH_g = 74\%$; $D_n = 10.0$ mm; bubble on/off ratio = 30 s/3 min).

may be because the slugging flow blocks the interfiber flow paths leading to local by-passing and uneven flow distribution, which counteracts the flux enhancement due to the negligibly intensified surface shear rate under a higher gas flow rate. As a result, the gas flow rate has little effect on the flux if it is higher than 1.2 $L{\cdot}min^{-1}$. Hence, there is a preferable gas flow rate for gas bubbling to achieve a higher enhancement in flux, and excessive increase of gas flow rate may damage the mechanical properties of fibers and increase energy consumption.

Furthermore, Figure 3 shows that the permeate flux increases with the increasing feed flow rate under the same gas flow rate. With the high Reynolds number ($Re$) caused by the increasing $Q_f$, a better turbulent effect appears to decrease the mass transfer coefficient and improve the hydrodynamics adjacent to the feed-side membrane surface, leading to the weaker temperature and concentration polarization phenomena. Consequently, relatively higher feed flow rate is better for bubbles' distribution over the membrane surface and generates flow disturbance in which the thermal boundary layer in the feed side may be reduced effectively, and hence the higher flux enhancement is obtained.

## Bubble relative humidity

The relationship between the flux enhancement ratio and the bubble relative humidity is plotted in Figure 4.

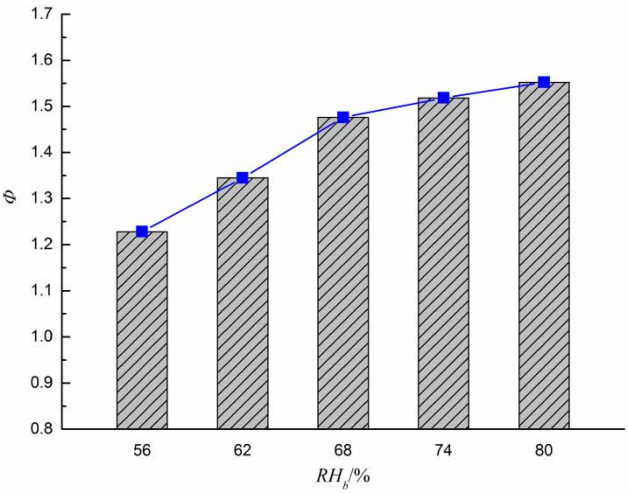


**Figure 4** | Effect of bubble relative humidity on trans-membrane flux (333 K saturated NaCl solution as feed: $T_{f\text{-}in} = 333$ K; $T_c = 283$ K; $Q_a = 0.84$ m$^3$·h$^{-1}$; $FF = 25.6\%$; $Q_g = 0.5$ L·h$^{-1}$; $D_n = 10.0$ mm; bubble on/off ratio = 30 s/3 min).

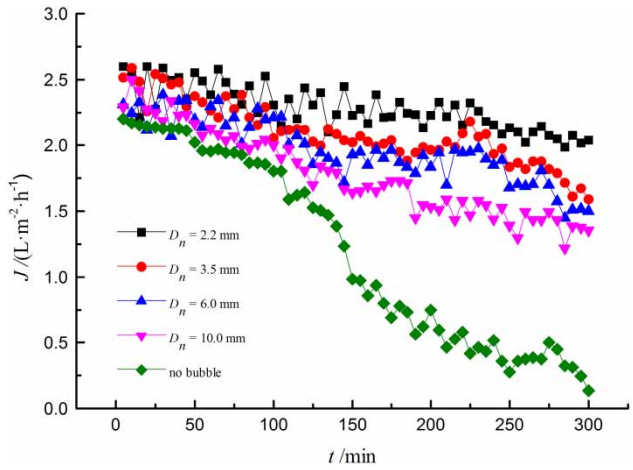


**Figure 5** | Effect of nozzle size on the enhancement of critical flux (333 K saturated NaCl solution as feed: $T_{f\text{-}in} = 333$ K; $T_c = 283$ K; $Q_a = 0.84$ m$^3$·h$^{-1}$; $FF = 25.6\%$; $Q_g = 0.5$ L·h$^{-1}$; $RH_g = 74\%$; bubble on/off ratio = 30 s/3 min).

The 60 min experiment is run at fixed parameters of $Q_g = 0.5$ L·h$^{-1}$, $D_n = 10.0$ mm, and bubble on/off ratio = 30 s/3 min.

It can be seen that the $\Phi$ value increases dramatically from 1.228 to 1.552 at a range of $RH_g$ from 58% to 80%. As the bubble relative humidity increases, small bubbles are not burst easily and tend to aggregate into the formation of gaseous mass. Subsequently, gaseous mass flows with the feed flow in the hot feed side to develop slug flow (intermittent large bullet-shaped bubbles with less clear phase boundaries). The better turbulent effect is caused by the slug flow, and then the shear intensity at the membrane surface increases. Thereby, better membrane permeate performance can be attained in a relatively higher relative humidity.

## Influence of nozzle size on bubble-assisted SGMD process

### The enhancement of critical flux

Figure 5 shows the comparison of the permeation flux vs. time with $D_n$ (0, 2.2, 3.5, 6.0, 10.0 mm) in an intermittent bubble-assisted system. Saturated NaCl solution (333 K) is chosen as the feed for 300 min in batch experiments.

As can be seen, the flux with two-phase flow is relatively larger than that with single flow throughout the experiments. Meanwhile, the permeate flux without injecting air in the feed stream decreases gradually with time. However, the fluxes maintain the relatively higher level at the beginning of the runs (0–110 min) with gas sparging. During 110–300 min, the flux is followed by a much slower decline with gas injection. At the point of 300 min, the flux drops essentially to zero (~0.13 L·m$^{-2}$·h$^{-1}$) without bubbling. Unlike the single-phase flow, the two-phase flow can not only promote local mixing near the membrane to displace the upper part of the polarization layer, but also increase the feed side cross-flow velocity, thus creating better fluid hydrodynamics. Consequently, a flux increase contributes to the gas injection. The reason for sudden flux drop in the non-bubbling case may be that NaCl crystals accumulate on the membrane surface when the feed is concentrated to a critical hyper-saturated state with increasing operating time, thus increasing the thermal resistance (i.e., temperature drop) gradually. Consequently, a dramatic major decline occurrence follows.

For two-phase flow, it is clear that a small $D_n$ is helpful to attain a higher trans-membrane flux. The flux increases from ~1.35 to ~2.04 L·m$^{-2}$·h$^{-1}$ with the declining $D_n$ from 10.0 to 2.2 cm at the end of the experimental operation. This may be because larger bubbles injected from the bigger nozzle result in local channeling (air bubble or bag blocking the flow of liquid in the channel) and uneven flow distribution. However, smaller bubbles induce the

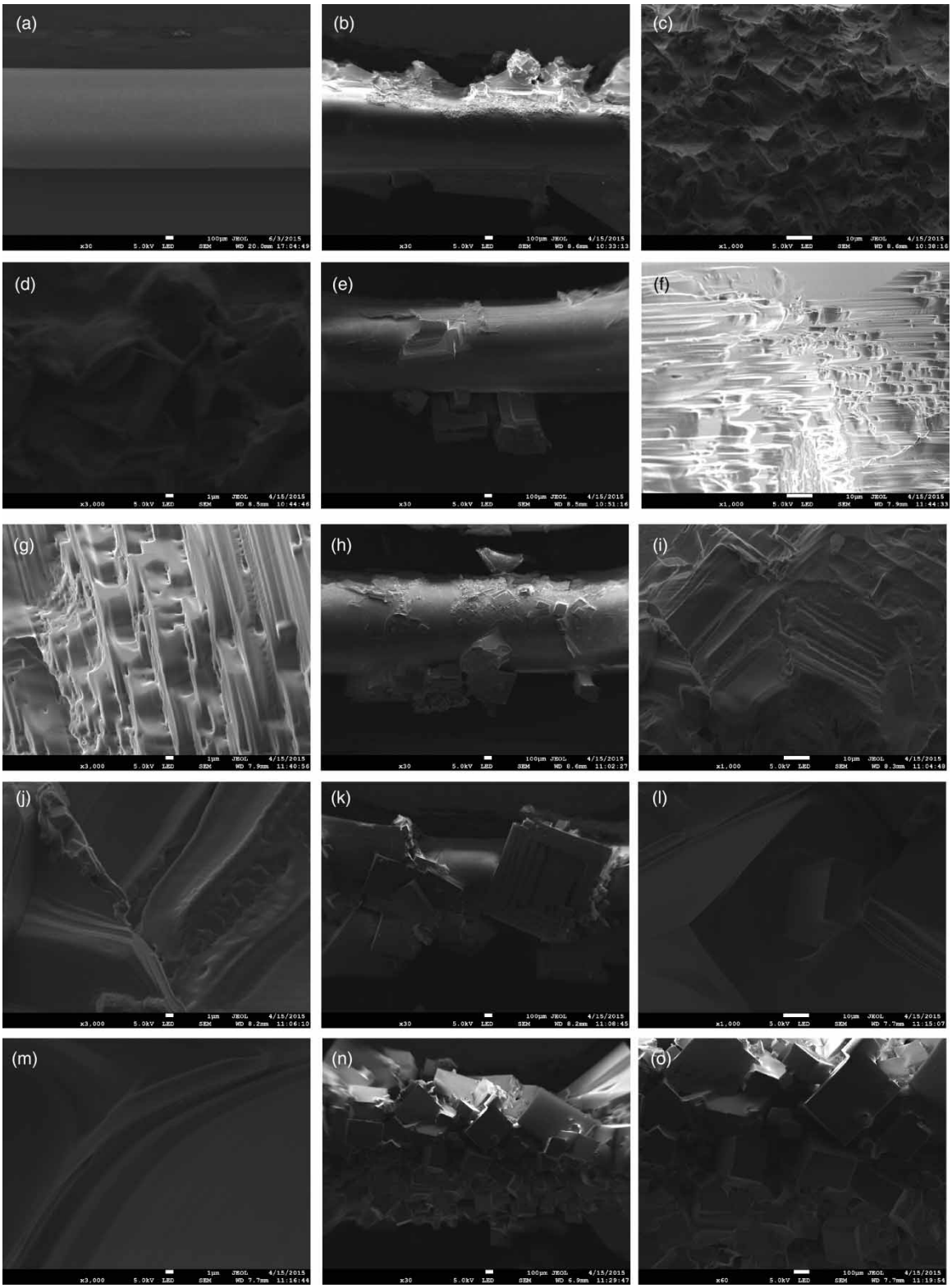


**Figure 6** | (a) SEM image of clean membrane; (b)–(o) SEM images of fouled membrane in high concentration intermittent bubble-enhanced SGMD at different nozzle sizes: (b)–(d) $D_n =$ 2.2 mm; (e)–(g) $D_n = 3.5$ mm; (h)–(j) $D_n = 6.0$ mm; (k)–(m) $D_n = 10.0$ mm; (n) and (o) $D_n = 0$ mm.

secondary flows and wakes, which enhances turbulence effect and the liquid convection. Additionally, the slug flow caused by smaller bubbles can form an annular falling film to create a high shear stress region. Therefore, it is necessary to identify the fine nozzle to avoid large bubbles to bring about superior evaporation performance in an incessant MD process.

### Scaling control

To further investigate the influence of gas bubbling with different $D_n$ on fouling control, the crystal deposition on the membrane surface is examined by SEM. Figure 6 shows SEM images of surfaces of membrane for six membrane systems: clean membrane, fouled membrane with gas–liquid two-phase flow ($D_n = 2.2,\ 3.5,\ 6.0,\ 10.0$ mm), and fouled membrane with single-phase flow.

In Figure 6(a), no crystal deposition is observed on the membrane surface for the fresh membrane. After 5 h operation, the membrane surface is almost completely covered with NaCl crystals for the non-bubbling case; while a relatively small amount of crystals are observed for the bubbling case. The physical observation of crystal deposition shows good agreement with the drastic flux decline presented in Figure 5. With gas sparging, moving slugs cause pressure pulsing in the liquid around them, which disrupts the concentration polarization layer. Also, the enhanced sheer stress can reduce the formation of crystals on the low membrane surface. Therefore, fouling limitation is improved by gas bubbling at the feed side in SGMD.

With the decrease of $D_n$, the fouling layer on the surface of the membrane is much thinner. Additionally, the scaling deposition is close to less uniform cubic crystals and the crystal face is much rougher. This is consistent with the tendency of flux decline with time. For smaller $D_n$, more falling films and bubble wakes can create the shear stress fluctuation in bubbling MD, which deters normal formation of NaCl crystals. Again, secondary flow induced by smaller bubbles is more helpful to erode the crystal attached on the membrane, leading to an uneven crystal surface. Hence, a gas sparging with smaller $D_n$ is confirmed to overcome the concentration polarization and greatly mitigate the membrane fouling.

## CONCLUSION

From this study, it was found that an intermittent gas flow seems to be more effective than a steady one under the same experimental operating conditions, even if it improves the flux in comparison with the one without bubbling. A higher enhancement ratio (1.518) could be obtained with the bubble on/off ratio of 30 s/3 min. Within certain bubble intervals, there is also an initial increase observed with the increase of gas flow rate. However, if the bubbling interval extends for too long, the fouling issue will be more serious. A further gas flow rate in permeate flux does not result in any further improvement in the permeate flux. In addition, a reasonably high bubble relative humidity of 80% is preferable for a higher flux enhancement ratio (1.623).

Experiments on a range of nozzle sizes have shown that slugs in MD hollow fibers by gas–liquid two-phase flow are very efficient to enhance permeate flux when limited by crystal deposition. Smaller nozzle size is more useful to enhance permeate flux and postpone a sharp flux decline. The results are consistent with the inspection of membrane surface autopsy by SEM. It is observed that less crystal deposition with rougher crystal face occurs on the membrane surface when using the smaller nozzle size (2.2 mm) in the intermittent gas bubbling experiment.

Regarding the conductivity and retention rate of permeate in SGMD, the repeat test indicated the good reproducibility of the permeate flux and high hydrophobic property with conductivity of over 19.2 $\mu s \cdot cm^{-1}$ and retention rate of over 99.7%.

To sum up, intermittent bubbling can not only improve the permeate flux, but also remove the deposited salt and foulants from the membrane surface. It is available to resist the fouling formation and deposition for a high concentration SGMD process.

## ACKNOWLEDGEMENTS

Thanks are given to the Department of Science & Technology of Hainan Province, P.R. China for program funding (217101, ZDKJ2016022, ZDYF2017011, 217100).

## REFERENCES


Calabro, V. & Drioli, E. 1997 Polarization phenomena in integrated reverse osmosis and membrane distillation for seawater desalination and waste water treatment. *Desalination* **108**, 81–82.

Cerón-Vivas, A., Morgan-Sagastume, J. M. & Noyola, A. 2012 Intermittent filtration and gas bubbling for fouling reduction in anaerobic membrane bioreactors. *J. Membr. Sci.* **423–424**, 136–142.

Chen, G. Z., Yang, X., Wang, R. & Fane, A. G. 2013 Performance enhancement and scaling control with gas bubbling in direct contact membrane distillation. *Desalination* **308**, 47–55.

Chen, G. Z., Yang, X., Lu, Y. H., Wang, R. & Fane, A. G. 2014 Heat transfer intensification and scaling mitigation in bubbling-enhanced membrane distillation for brine concentration. *J. Membr. Sci.* **470**, 60–69.

Cui, Z. F., Chang, S. & Fane, A. G. 2003 The use of gas bubbling to enhance membrane processes. *J. Membr. Sci.* **221**, 1–35.

Ding, Z. W., Liu, L. Y., Liu, Z. & Ma, R. Y. 2011 The use of intermittent gas bubbling to control membrane fouling in concentrating TCM extract by membrane distillation. *J. Membr. Sci.* **372**, 172–181.

Edwie, F. & Chung, T. S. 2012 Development of hollow fiber membranes for water and salt recovery from highly concentrated brine via direct contact membrane distillation and crystallization. *J. Membr. Sci.* **421–422**, 111–123.

Eykens, L., De Sitter, K., Dotremont, C., Pinoy, L. & Van der Bruggen, B. 2017 Membrane synthesis for membrane distillation: a review. *Sep. Purif. Technol.* **182**, 36–51.

García, J. V., Dow, N., Milne, N., Zhang, J. H., Naidoo, L., Gray, S. & Duke, M. 2018 Membrane distillation trial on textile wastewater containing surfactants using hydrophobic and hydrophilic-coated polytetrafluoroethylene (PTFE) membranes. *Membranes (Basel)* **8**, 5–15.

Gryta, M., Tomaszewska, M., Grzechulska, J. & Morawski, A. W. 2001 Membrane distillation of NaCl solution containing natural organic matter. *J. Membr. Sci.* **181**, 279–287.

Guibert, D., Ben Aim, R., Rabie, H. & Côté, P. 2002 Aeration performance of immersed hollow-fiber membranes in a bentonite suspension. *Desalination* **148**, 395–400.

Hickenbottom, K. L. & Cath, T. Y. 2014 Sustainable operation of membrane distillation for enhancement of mineral recovery from hypersaline solutions. *J. Membr. Sci.* **454**, 426–435.

Jansen, A. E., Assink, J. W., Hanemaaijer, J. H., van Medevoort, J. & van Sonsbeek, E. 2013 Development and pilot testing of full-scale membrane distillation modules for deployment of waste heat. *Desalination* **323**, 55–65.

Lawson, K. W. & Lloyd, D. R. 1997 Membrane distillation. *J. Membr. Sci.* **124**, 1–25.

Liu, Y. F., Xiao, T. H., Bao, C. H., Zhang, J. F. & Yang, X. 2018 Performance and fouling study of asymmetric PVDF membrane applied in the concentration of organic fertilizer by direct contact membrane distillation (DCMD). *Membranes (Basel)* **8**, 2–13.

Lu, Y., Ding, Z. W., Liu, L. Y., Wang, Z. J. & Ma, R. Y. 2008 The influence of bubble characteristics on the performance of submerged hollow fiber membrane module used in microfiltration. *Sep. Sci. Technol.* **61**, 89–95.

Nghiem, L. D. & Cath, T. 2011 A scaling mitigation approach during direct contact membrane distillation. *Sep. Purif. Technol.* **80**, 315–322.

Quist-Jensen, C. A., Ali, A., Mondal, S., Macedonio, F. & Drioli, E. 2016 A study of membrane distillation and crystallization for lithium recovery from high-concentration aqueous solutions. *J. Membr. Sci.* **505**, 167–173.

Schofield, R. W., Fane, A. G. & Fell, C. J. D. 1987 Heat and mass transfer in membrane distillation. *J. Membr. Sci.* **33**, 299–313.

Tijing, L. D., Woo, Y. C., Choi, J. S., Lee, S., Kim, S. H. & Shon, H. K. 2015 Fouling and its control in membrane distillation – A review. *J. Membr. Sci.* **475**, 215–244.

Wibisono, Y., Cornelissen, E. R., Kemperman, A. J. B., van der Meer, W. G. J. & Nijmeijer, K. 2014 Two-phase flow in membrane process: a technology with a future. *J. Membr. Sci.* **453**, 566–602.

Wu, C. R., Li, Z. G., Zhang, J. H., Jia, Y., Gao, Q. J. & Lu, X. L. 2015 Study on the heat and mass transfer in air-bubbling enhanced vacuum membrane distillation. *Desalination* **373**, 16–26.


First received 25 December 2018; accepted in revised form 14 March 2019. Available online 24 April 2019